European Journal of Orthodontics 31 (2009) 129–134
doi:10.1093/ejo/cjn088
Advance Access publication 23 December 2008

Accuracy of three-dimensional measurements obtained from cone beam computed tomography surface-rendered images for cephalometric analysis: influence of patient scanning position

Bassam Hassan, Paul van der Stelt and Gerard Sanderink
Department of Oral Radiology, Academic Centre for Dentistry Amsterdam (ACTA), The Netherlands

SUMMARY The aims of this study were to assess the accuracy of linear measurements on three-dimensional (3D) surface-rendered images generated from cone beam computed tomography (CBCT) in comparison with two-dimensional (2D) slices and 2D lateral and postero-anterior (PA) cephalometric projections, and to investigate the influence of patient head position in the scanner on measurement accuracy. Eight dry human skulls were scanned twice using NewTom 3G CBCT in an ideal and a rotated position and the resulting datasets were used to create 3D surface-rendered images, 2D tomographic slices, and 2D lateral and PA projections. Ten linear distances were defined for cephalometric measurements. The physical and radiographic measurements were repeated twice by three independent observers and were compared using repeated measures analysis of variance ($P = 0.05$). The radiographic measurements were also compared between the ideal and the rotated scan positions.

The radiographic measurements of the 3D images were closer to the physical measurements than the 2D slices and 2D projection images. No statistically significant difference was found between the ideal and the rotated scan measurements for the 3D images and the 2D tomographic slices. A statistically significant difference ($P < 0.001$) was observed between the ideal and rotated scan positions for the 2D projection images. The findings indicate that measurements based on 3D CBCT surface images are accurate and that small variations in the patient's head position do not influence measurement accuracy.

Introduction

Two-dimensional (2D) projection radiographs have been traditionally considered the modality of choice for the assessment of craniofacial structures for orthodontic cephalometric analysis. However, the superimposition of structures of the left and right side of the skull, the unequal enlargement ratios of the left and right side, and the possible distortion of the mid-facial structures are well-recognized shortcomings of this imaging technique (Chen *et al.*, 2004; Bruntz *et al.*, 2006). This led to the development of alternative cephalometric analysis approaches. The most recent method is three-dimensional (3D) cephalometry in which the linear and angular measurements are made directly on 3D surface and volume-rendered images obtained from computed tomography (CT) scans (Halazonetis, 2005; Park *et al.*, 2006). The accuracy of these 3D-rendered images has been previously evaluated and the findings showed that direct 3D measurements are highly accurate with no significant discrepancies from physical measurements (Cavalcanti and Vannier, 1998; Cavalcanti *et al.*, 2004). However, the relatively high radiation dose, costs, and limited availability associated with CT scans impede its adoption to routine clinical orthodontic diagnosis and treatment planning (Kau *et al.*, 2005).

Cone beam computed tomography (CBCT) has emerged as a promising technology with the potential to replace CT as the method of choice for 3D cephalometric analysis as it provides tomographic views and volumetric reconstructions at substantially reduced radiation doses and expense (Swennen and Schutyser, 2006). CBCT has become a frequently utilized imaging modality in clinical orthodontics, implant planning, temporomandibular joint imaging, and maxillofacial surgery (Walker *et al.*, 2005; Sakabe *et al.*, 2006).

There are several types of radiographic images which can be generated from CBCT data including 2D tomographic multi-planar reformatted (MPR) slices, 2D virtual lateral and postero-anterior (PA) cephalometric projections, 3D surface and volume-rendered images, and panoramic reconstruction. Several reports have established the accuracy of linear measurements of different CBCT systems based on 2D tomographic slices and 2D virtual lateral cephalographic images (Lascala *et al.*, 2004; Hilgers *et al.*, 2005; Kumar *et al.*, 2007; Ludlow *et al.*, 2007). However, the accuracy of linear measurements based on 3D surface and volume-rendered CBCT images is still to be assessed. Due to the dissimilarity in the image acquisition methodology, reconstruction algorithms, and detector characteristics, CBCT reconstructed 3D surface-rendered images of the maxillofacial region are inferior in quality in comparison with CT (Loubele *et al.*, 2006). This raises questions regarding the accuracy of CBCT 3D-rendered models for direct 3D cephalometry.

In practice, the position of the patient's head during the scanning procedure could deviate from a true vertical and horizontal orientation. It is therefore important not only to assess the accuracy of craniofacial measurements on 3D surface bone models generated from CBCT scans in ideal scanning settings, but also to examine the influence of head positioning during the scanning procedure on the accuracy of the measurements. It is also necessary to investigate whether a retrospective correction of the patient scanning position using software tools as previously suggested (Swennen and Schutyser, 2006) is required. The influence of head position in the scanner on the accuracy of measurements of the mandibular anatomy based on CBCT 2D axial slices and panoramic reconstructions has been reported. The results showed that head position did not have a significant influence on measurement accuracy (Moshiri *et al.*, 2007).

The aims of this study were to assess the accuracy of linear measurements on 3D surface-rendered images generated from CBCT datasets and to compare them with those made on 2D tomographic slices and on 2D lateral and PA cephalometric projections. The influence of head position of the patient in the scanner on measurement accuracy for the three image types was also evaluated to establish recommendations for CBCT in orthodontic practice.

Materials and methods

Physical measurements

Eight dry human skulls, which were not identified by gender, age, or ethnicity, were used in the study. To undertake the measurements 10 linear distances were selected in the maxilla and mandible. The selected lines were orientated horizontally, vertically, and obliquely to account for linear measurements made in all three dimensions. The gold standard was obtained for each of the 10 lines by physical measurements using a digital calliper with an accuracy of 0.01 mm (Gamma, Amsterdam, The Netherlands). The physical measurements were repeated twice by three independent observers. (Table 1)

Radiographic scan

The radiographic scans were obtained using the NewTom 3G CBCT system (Quantitative Radiology, Verona, Italy). Each skull was placed in a plastic box with the mid-sagittal plane coinciding with that of the box. The skull was then fixed in the box using dental wax and wrapped in plastic sheets. The box was filled with water. The skulls were kept dry during the scan to avoid possible expansion due to absorption of water which can influence measurement accuracy.

The skulls were positioned according to the recommendations of the CBCT manufacturer with the Frankfort plane perpendicular to the floor. Each skull was scanned twice: first in an 'ideal' position and second in a 'rotated' position. The rotated scan was obtained by placing a wooden wedge under the right edge of the box and rotating the plastic box around the *Z* scanning axis by approximately 15–18 degrees. The scans were later checked using the software tools to ensure consistency in skull rotation angle and orientation. (Figure 1)

The imaging parameters were 3.24 mAs, 110 kVp, and a 20 second scan time using the 9 inch detector field. The raw data were reconstructed using the high-resolution reconstruction algorithm setting provided by the CBCT software (QR NNT v2.0.4, Quantitative Radiology). The resulting volume had an isotropic voxel size of 0.25 mm and the datasets were exported as 512 × 512 matrices in DICOM 3 file format and saved on an external hard disk.

Table 1 Physical measurements of the gold standard (all measurements are given in mm; standard deviation in brackets).

Anatomical landmarks										
Skull number	Maxillary landmarks				Mandibular landmarks					
	Orbital(L)-orbital(R)	Orbital(L)-anterior nasal spine	Orbital(R)-anterior nasal spine	Anterior nasal spine-posterior nasal spine	Condyle(L)-condyle(R)	Coronoid(L)-coronoid(R)	Condyle(L)-coronoid(L)	Condyle(R)-coronoid(R)	Condyle(L)-coronoid(R)	Condyle(R)-coronoid(L)
1	73.69 (0.16)	43.73 (0.16)	45.71 (0.11)	50.40 (0.22)	81.54 (0.26)	85.94 (0.27)	30.02 (0.09)	27.22 (0.09)	90.26 (0.11)	86.51 (0.12)
2	71.62 (0.15)	46.81 (0.08)	43.83 (0.11)	54.21 (0.11)	99.77 (0.48)	95.48 (0.09)	26.92 (0.22)	27.61 (0.12)	99.69 (0.14)	102.75 (0.07)
3	80.29 (0.10)	47.30 (0.13)	53.12 (0.10)	55.35 (0.14)	90.14 (0.29)	81.93 (0.19)	34.58 (0.12)	33.21 (0.13)	91.90 (0.04)	93.59 (0.12)
4	74.31 (0.12)	43.48 (0.19)	47.12 (0.25)	51.55 (0.17)	87.82 (0.13)	85.65 (0.11)	27.74 (0.14)	26.97 (0.05)	91.09 (0.14)	90.71 (0.25)
5	64.12 (0.13)	39.61 (0.27)	41.04 (0.15)	46.39 (0.34)	88.78 (0.16)	81.62 (0.12)	34.08 (0.19)	34.57 (0.19)	91.46 (0.06)	91.46 (0.11)
6	66.05 (0.45)	41.59 (0.13)	39.75 (0.37)	48.73 (0.26)	85.94 (0.13)	79.83 (0.05)	30.33 (0.16)	30.00 (0.20)	87.45 (0.21)	88.86 (0.19)
7	59.27 (0.13)	38.75 (0.13)	40.20 (0.14)	43.47 (0.19)	108.81 (0.13)	90.71 (0.09)	38.01 (0.13)	40.26 (0.07)	105.89 (0.15)	107.37 (0.09)
8	61.27 (0.33)	38.75 (0.12)	36.41 (0.08)	45.55 (0.22)	97.14 (0.19)	94.23 (0.09)	34.04 (0.06)	31.69 (0.09)	101.90 (0.23)	100.34 (0.27)

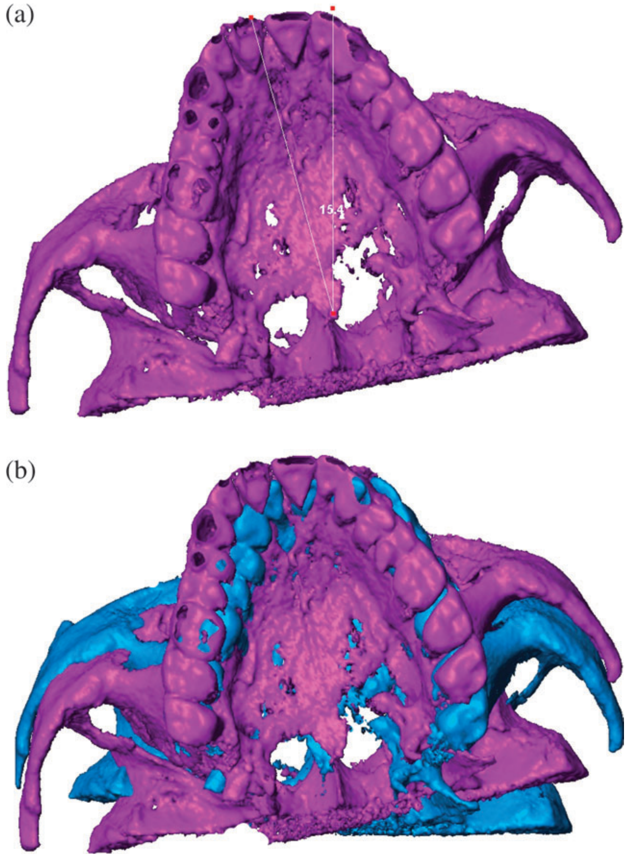

Figure 1 Three-dimensional surface-rendered model of the maxilla shown with a rotation angle of 15.4 degrees (a) (the left line represents the true mid-sagittal plane when the skull is in an ideal scanning position and the right line the deviation from true mid-sagittal when the skull is rotated) and in an ideal (blue) and rotated (purple) position superimposed on each other (b).

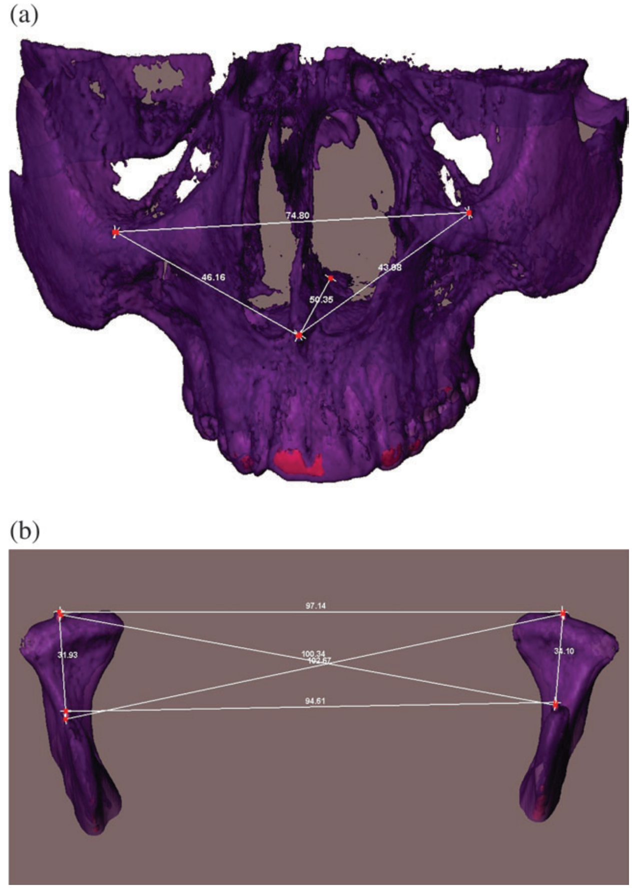

Figure 2 Linear measurements on the three-dimensional surface-rendered model of (a) maxilla: between OI(R)-OI(L), ANS-PNS, OI(R)-ANS, and OI(L)-ANS and (b) mandible: between Con(R)-Con(L), Cor(R)-Cor(L), Con(R)-Cor(R), Con(L)-Cor(L), Con(R)-Cor(L), and Con(L)-Cor(R).

Radiographic measurements

The DICOM datasets were imported into commercial software (Amira v.4.2, Mercury Computer Systems, Chelmsford, Massachusetts, USA) for analysis. Each skull dataset was processed to create three types of images; 3D surface-rendered images of the maxilla and mandible (Figure 2), 2D tomographic MPR slices with a thickness of 0.5 mm (Figure 3), and 2D lateral and PA projections. (Figure 4).

The original scan position was left unchanged with no corrections. The 3D surface models were created automatically in the software by specifying a single threshold grey level value of an average of 650 ± 50 for the mandible and 450 ± 30 for the maxilla. Different values for the maxilla and mandible were used because of the difference in bone thickness and density between the maxilla and mandible which influence the bone surface rendering quality and the visibility of the anatomical landmarks. The condylar head showed some artefacts which had to be corrected manually using segmentation tools available in the software.

The 2D lateral and PA projections were created using orthographic 1:1 true scale and a reference system was established in the X, Y, and Z directions.

The 2D and 3D measurement tools in Amira are calibrated by the software manufacturer to produce length measurements expressed as millimeters with an accuracy of 0.01 mm. Three observers were trained to use the software for this study. Each observer repeated the radiographic measurements twice for each image type for both scan positions (ideal and rotated) independently which resulted in a total of 12 radiographic measurements per line, per skull per observer (3×2 ideal + 3×2 rotated). The total number of radiographic measurements for the three observers for the eight skulls was 2880.

Statistical analysis

The accuracy of the gold standard for the selected distances was established by averaging the physical measurements of the three observers. The mean of each radiographic measurement for each image type was compared with the

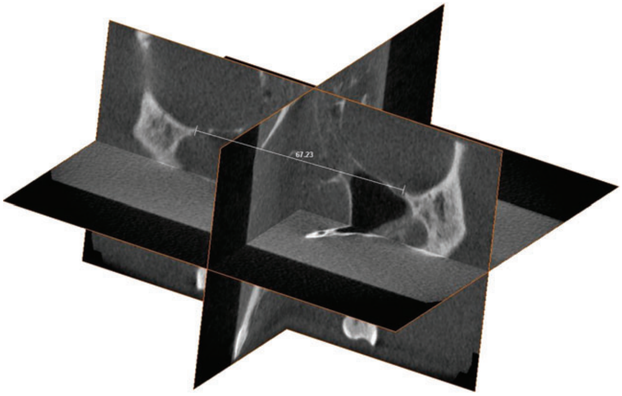

Figure 3 Two-dimensional multi-planar reformatted slices with a thickness of 0.5 mm (axial, coronal 'frontal' and sagittal). Linear measurement between OI(R) and OI(L).

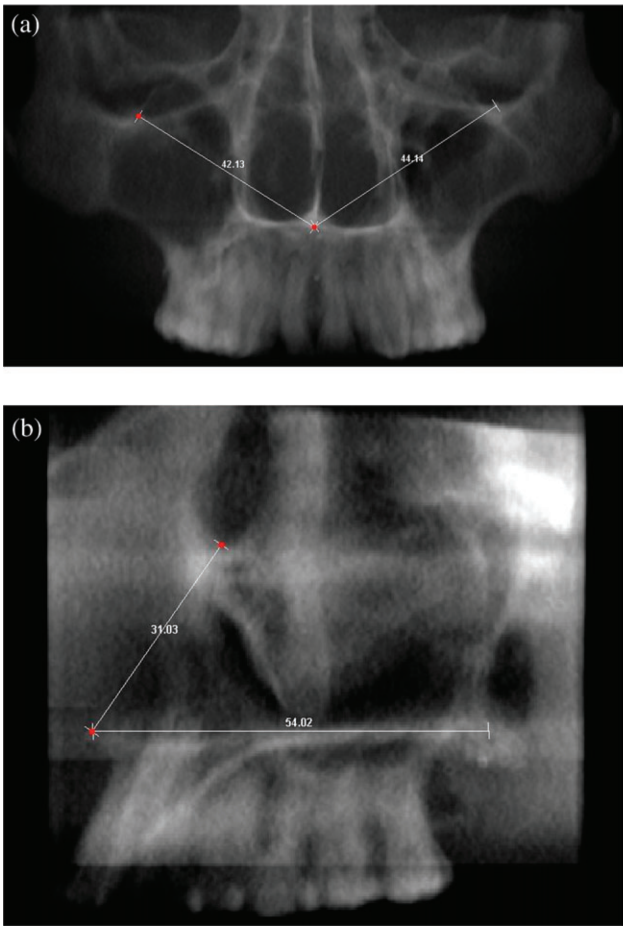

Figure 4 Linear measurements on two-dimensional radiographs. (a) Postereo-anterior projection: between OI(R)-ANS and OI(L)-ANS. (b) Lateral cephalogram: between ANS-PNS OI-ANS.

mean of the gold standard using analysis of variance of repeated measurements with the Statistical Package for Social Sciences version 14, (SPSS Inc., Chicago, Illinois, USA). The significance level was set to $P \leq 0.05$. Corresponding image types were assessed for both scan positions to minimize the influence of the interaction effect on the statistical results.

Results

The gold standard measurements are summarized in Table 1. The accuracy of the gold standard measurements was within 0.5 mm as the largest standard deviation (SD) was 0.48 mm. All radiographic measurements in both scan positions (ideal and rotated) were statistically different from the gold standard measurements at $P = 0.05$. However, as not all the differences were equal and some were relatively small, it can be argued that their relevance in clinical practice is limited.

In the ideal position, the largest observed difference between the mean 3D models and gold standard measurements was less than 0.5 mm [mean deviation (MD) = 0.39 mm, SD = 0.29], for 2D tomographic slices, the largest observed difference with the gold standard measurements was less than 1.0 mm (MD = 0.37 mm, SD = 0.84), and for 2D cephalometric (lateral and PA) projection images, less than 5 mm (MD = 4.1 mm, SD = 2.23).

The measurements in the rotated position were compared with the optimal position measurements for each image type. For 3D surface images and 2D tomographic slices, no statistically significant differences were found between the optimal and rotated scan data ($P = 0.73$ and $P = 0.93$, respectively). For 2D cephalometric lateral and PA projections, a statistically significant difference ($P < 0.001$) was observed between both scan positions (e.g. IO(R)-ANS line) (Table 2).

Discussion

This study was performed to investigate the effect of image type and patient head positioning on the accuracy of CBCT measurements for cephalometric analysis. For scanning positions (ideal and rotated), the difference between the 3D surface image measurements and the gold standard was relatively small (within 0.5 mm). This may be due to the fact that hard tissue transformations are rigid in nature, so scan position does not influence the location of the anatomical landmarks relative to each other. It is noteworthy though that soft tissue transformation is not necessarily rigid when the patient is positioned incorrectly in the scanner which may influence the outcome of the measurements. However, this could not be assessed as dry skulls were used in this research.

The difference between 2D tomographic slice measurements and the gold standard was also small (within 1.0 mm) in both scan positions and the findings are consistent with previous studies (Lascala *et al.*, 2004; Hilgers *et al.*, 2005; Kumar *et al.*, 2007; Ludlow *et al.*, 2007). However, the problems with 2D tomographic slices remain that

Table 2 Mean absolute differences (and standard deviations) of radiographic measurements and the gold standard for the selected distances.

Anatomical landmarks	Scan position					
	Optimal scan position			Rotated scan position		
	3D models	2D tomographic slices	2D cephalometric (lateral and PA) projections	3D models	2D tomographic slices	2D cephalometric (lateral and PA) projections
Orbital(L)-orbital(R)	0.39 (0.29)	0.34 (0.24)	0.37 (0.22)	0.43 (0.30)	0.66 (0.61)	**2.25 (2.59)**
Orbital(L)-anterior nasal spine	0.18 (0.18)	0.37 (0.84)	**3.53 (1.95)**	0.22 (0.11)	0.44 (0.44)	**3.97 (1.01)**
Orbital(R)-anterior nasal spine	0.22 (0.20)	0.33 (0.62)	**4.1 (2.23)**	0.27 (0.22)	0.31 (0.24)	**9.27 (4.36)**
Anterior nasal spine-posterior nasal spine	0.26 (0.25)	0.27 (0.26)	0.29 (0.32)	0.33 (0.46)	0.30 (0.51)	**1.78 (1.28)**
Condyle(L)-condyle(R)	0.22 (0.15)	0.15 (0.12)	0.17 (0.12)	0.18 (0.12)	0.15 (0.10)	**12.73 (2.55)**
Coronoid(L)-coronoid(R)	0.16 (0.11)	0.11 (0.09)	0.10 (0.08)	0.15 (0.10)	0.12 (0.07)	**12.42 (1.83)**
Condyle(L)-coronoid(L)	0.12 (0.10)	0.11 (0.08)	0.25 (0.36)	0.10 (0.77)	0.10 (0.07)	**5.71 (2.22)**
Condyle(R)-coronoid(R)	0.10 (0.08)	0.16 (0.10)	0.34 (0.28)	0.10 (0.14)	0.13 (0.09)	**2.93 (1.26)**
Condyle(L)-coronoid(R)	0.11 (0.06)	0.13 (0.32)	**3.21 (1.33)**	0.11 (0.17)	0.13 (0.41)	**6.06 (4.11)**
Condyle(R)-coronoid(L)	0.14 (0.08)	0.19 (0.22)	**4.08 (2.21)**	0.14 (0.16)	0.21 (0.11)	**6.97 (4.68)**

Differences of >1 mm between the radiographic measurements and the gold standard are shown in **bold.**
Differences of >1 mm for the 2D cephalometric measurements between the ideal and rotated scan position are underlined.

typically the two anatomical landmarks between which a line is drawn are not identifiable on the same slice when thin slices are utilized (0.5–1.0 mm). This is due to variations in the location of anatomical landmarks and also because of patient positioning errors. As such, it necessitates scrolling through the slices back and forth or right and left to identify the anatomical landmarks on both sides bilaterally or antero-posteriorly. This complicates the measurement process and typically requires more time and effort and can be considered inappropriate for cephalometric analysis.

Virtual lateral cephalograms and PA projections reconstructed from CBCT scan data have gained increasing popularity in recent years and are routine in the diagnostic report for each CBCT orthodontic patient. However, the results presented show that the measurements based on virtual lateral and PA cephalograms for some measurements (obliquely defined lines) deviated from the gold standard by more than 1 mm even when the scan was in an optimal position (Table 2).

When the skulls were rotated, a larger difference of more than 10 mm was found, which means that virtual cephalometric projection images created from CBCT data are sensitive to small variations in patient scanning position. virtual 2D projection images measurements were the least accurate among the three image types.

The accuracy of the radiographic measurements was limited by the voxel size employed (0.25 mm) and by the ability of the observer in determining the exact position of the anatomical landmarks. It is also possible that the rotation angle used in this study did not reflect the 'real' average patient positioning error in the CBCT apparatus, but no information could be found in the literature with regard to the incidence and extent of patient positioning errors in a scanner. Patient positioning discrepancies occur in all three dimensions (x, y, z). However, in this study only the influence of angular rotation around the z-axis on measurement accuracy was assessed.

Conclusions

Small variations in patient head position when a CBCT examination is performed do not affect the accuracy of linear measurements based on 3D surface-rendered models. The measurements based on 2D tomographic slices are also accurate but there is an increase in observer time and more effort is required to identify the anatomical landmarks using 2D slices; thus, from the point of view of an orthodontist, it might be considered impractical for cephalometric analysis.

Linear measurements based on 2D virtual lateral and PA projections were sensitive to small variations in head position which means that retrospective correction for patient position using software tools is required as was previously suggested if 2D virtual cephalograms are to be used for tracing (Swennen and Schutyser, 2006). This raises issues regarding how accurate an orthodontist can compensate for an incorrectly positioned patient in the absence of automatic software tools to perform this task.

When introducing protocols for 3D analysis with CBCT images in orthodontics, it is important to emphasize the advantages and limitations of the different visualization techniques available with this imaging modality. The results of this study suggest that performing cephalometric analysis on 3D-rendered models seems to be the most appropriate approach with regard to accuracy and convenience.

Address for correspondence

Bassam Hassan
Department of Oral Radiology
ACTA
Louwesweg 1
1066EA Amsterdam
The Netherlands
E-mail: bhassan@acta.nl

Acknowledgement

We would like to thank Dr Hans Verheij for carrying out the statistical analysis and for his scientific support.

References

Bruntz L Q, Palomo J M, Baden S, Hans M G 2006 A comparison of scanned lateral cephalograms with corresponding original radiographs. American Journal of Orthodontics and Dentofacial Orthopedics 130: 340–348

Cavalcanti M G, Vannier M W 1998 Quantitative analysis of spiral computed tomography for craniofacial clinical applications. Dentomaxillofacial Radiology 27: 344–350

Cavalcanti M G, Rocha S S, Vannier M W 2004 Craniofacial measurements based on 3D-CT volume rendering: implications for clinical applications. Dentomaxillofacial Radiology 33: 170–176

Chen Y J, Chen S K, Yao J C, Chang H F 2004 The effects of differences in landmark identification on the cephalometric measurements in traditional versus digitized cephalometry. Angle Orthodontist 74: 155–161

Halazonetis D J 2005 From 2-dimensional cephalograms to 3-dimensional computed tomography scans. American Journal of Orthodontics and Dentofacial Orthopedics 127: 627–637

Hilgers M L, Scarfe W C, Scheetz J P, Farman A G 2005 Accuracy of linear temporomandibular joint measurements with cone beam computed tomography and digital cephalometric radiography. American Journal of Orthodontics and Dentofacial Orthopedics 128: 803–811

Kau C H, Richmond S, Palomo J M, Hans M G 2005 Three-dimensional cone beam computerized tomography in orthodontics. Journal of Orthodontics 32: 282–293

Kumar V, Ludlow J B, Mol A, Cevidanes L 2007 Comparison of conventional and cone beam CT synthesized cephalograms. Dentomaxillofacial Radiology 36: 263–269

Lascala C A, Panella J, Marques M M 2004 Analysis of the accuracy of linear measurements obtained by cone beam computed tomography (CBCT-NewTom). Dentomaxillofacial Radiology 33: 291–294

Loubele M, Maes F, Schutyser F, Marchal G, Jacobs R, Suetens P 2006 Assessment of bone segmentation quality of cone-beam CT versus multislice spiral CT: a pilot study. Oral Surgery, Oral Medicine, Oral Pathology, Oral Radiology, and Endodontology 102: 225–234

Ludlow J B, Laster W S, See M, Bailey L J, Hershey H G 2007 Accuracy of measurements of mandibular anatomy in cone beam computed tomography images. Oral Surgery, Oral Medicine, Oral Pathology, Oral Radiology, and Endodontology 103: 534–542

Moshiri M, Scarfe W C, Hilgers M L, Scheetz J P, Silveira A M, Farman A G 2007 Accuracy of linear measurements from imaging plate and lateral cephalometric images derived from cone-beam computed tomography. American Journal of Orthodontics and Dentofacial Orthopedics 132: 550–560

Park S H, Yu H S, Kim K D, Lee K J, Baik H S 2006 A proposal for a new analysis of craniofacial morphology by 3-dimensional computed tomography. American Journal of Orthodontics and Dentofacial Orthopedics 129: 623–634

Sakabe R, Sakabe J, Kuroki Y, Nakajima I, Kijima N, Honda K 2006 Evaluation of temporomandibular disorders in children using limited cone-beam computed tomography: a case report. Journal of Clinical Pediatric Dentistry 31: 14–16

Swennen G R J, Schutyser F 2006 Three-dimensional cephalometry: spiral multi-slice vs cone-beam computed tomography. American Journal of Orthodontics and Dentofacial Orthopedics 130: 410–416

Walker L, Enciso R, Mah J 2005 Three-dimensional localization of maxillary canines with cone-beam computed tomography. American Journal of Orthodontics and Dentofacial Orthopedics 128: 418–423